

# Theoretical methods for the determination of mixing

BAOLIAN CHENG,<sup>1</sup> JAMES GLIMM,<sup>2,3</sup> HYEONSEONG JIN,<sup>2</sup> AND DAVID SHARP<sup>1,4</sup>

<sup>1</sup>Applied Physics Division, Los Alamos National Laboratory, Los Alamos, New Mexico

<sup>2</sup>Department of Applied Mathematics and Statistics, Stony Brook University, Stony Brook, New York

<sup>3</sup>Center for Data Intensive Computing, Brookhaven National Laboratory, Upton, New York

<sup>4</sup>Theoretical Division, Los Alamos National Laboratory, Los Alamos, New Mexico

(RECEIVED 10 October 2002; ACCEPTED 4 April 2003)

## Abstract

Acceleration-driven fluid mixing is studied here from a theoretical point of view. Considerable progress has been achieved in the understanding of mix. Theories of the authors are reviewed that allow prediction of the edge of the mixing zone, in agreement with experimental data. Theories that describe the distribution of masses within the mixing region are also reviewed. The theory we present describes a chunk mix regime, in which two phases are mixed at a chunk level, but for which there is no atomic mixing. Thus the two phases are segregated into disjoint regions of space.

**Keywords:** Mixing; Multiphase flow; Rayleigh–Taylor instability

## 1. INTRODUCTION

Characterization of mixing rates for acceleration-driven flows is important for the design of inertial confinement (ICF) targets and the study of astrophysical flows modeling supernovae and geophysical flows involving thermal inversion or density inversion (e.g., a salt dome) layers. Under-prediction of mixing rates from many simulation codes relative to experiments and observational data adds to the importance of a theoretical investigation. Remarkably, the theoretically predicted mixing rates have been in agreement with experiment for some time. In this article we summarize our main results for the theoretical determination of mixing rates, with an emphasis on recent improvements that add considerably to the power and applicability of these methods. We use these mixing rates to parameterize a subgrid mixing model, also presented here. Detailed analytic solutions to this model have been known for some time. We present the weakly compressible asymptotic expansion (the incompressible limit). We comment on the relation of our results to the direct simulation determination of mixing rates.

The outline of our approach can be summarized as:

1. Bubble merger models to predict bubble growth rate;
2. Characterization of the center of mass (COM) motion to link bubble side mix predictions to spike side mix predictions;

3. Determination of drag as a function of Atwood number, so that arbitrary accelerations can be studied;
4. Analytic determination of leading and below leading order large time asymptotics for the edge motion equations;
5. Mix model (subgrid model) equations;
6. Determination of an effective diffusion and Reynolds stress term for use in reduced models.

## 2. BUBBLE MERGER MODELS

Bubble merger models predict the penetration rate of fingers of light fluid (bubbles) into the heavy fluid. For acceleration-driven mixing, it is observed that the bubbles increase in size, through a process of bubble competition and merger.

In this process, advanced bubbles are accelerated relative to the mean bubble motion, whereas retarded ones are held back. Thus the smaller bubbles (also generally the retarded ones) become removed from the interface of advancing bubbles, whereas the larger, advanced ones expand to fill the resulting space. Sharp and Wheeler (1961) proposed a model to describe this process. The model was corrected by Glimm and Sharp (1990, 1997) to include the hydrodynamical accelerations (positive and negative) given to advanced and retarded bubbles due to their positions relative to the mean bubble penetration height. Such models were extended to three dimensions by Oron *et al.* (2001) and independently by Cheng *et al.* (2002a), with improved predictions. The three-dimensional (3D) models predict not only the growth rates for the bubble interface (both agree with experiment;

Address correspondence and reprint requests to: James Glimm, Department of Applied Mathematics and Statistics, Stony Brook University, Stony Brook, NY 11794-3600, USA. E-mail: glimm@ams.sunysb.edu

Cheng *et al.* is slightly higher), they also predict the bubble height-to-width ratio. For this quantity, the two models are distinctly different in their predictions (see Table 1). Agreement of the Cheng *et al.* model with experimental data is very satisfactory.

The bubble dynamic equations are formulated in scaled variables, from which the  $Ag t^2$  dynamic growth has been removed. This being the case, the self-similar, late time solution appears as a fixed point. In fact, it is a renormalization group (RNG) fixed point.

For steady acceleration, that is, Rayleigh–Taylor (RT) mixing, the bubble penetration height  $h_b$  satisfies the scaling law  $h_b = \alpha_b Ag t^2$ . Four directly measurable quantities determine the growth rate constant  $\alpha_b$  in this formula. The measurements, the relation of these quantities to  $\alpha_b$ , and the experimental validation of this relation are contained in Cheng *et al.* (2002a). We list the four quantities: (1) Let  $t'_m$  be the time to merger for a pair of interacting bubbles. Then  $\omega = \langle 1/t'_m \rangle_*$  is the mean inverse time to merger, and thus the mean merger rate. It is evaluated at the fixed point, (2)  $h'_m$  is the maximum height separation, that is, the height for instantaneous merger, (3)  $c_b$  is the speed of a single bubble in a periodic array, and (4)  $k$  is a geometrical factor giving the increase in radius for a single merger event, slightly less than  $\frac{1}{2}$ . Each of the proceeding is expressed in scaled units. Then the fixed point formula for  $\alpha_b$  is

$$\alpha_b = \frac{k}{4} \left( c_b + \frac{1+k}{2} h'_m \omega \right) \omega. \tag{1}$$

As written, the equation has been verified by direct comparison to experimental data (Cheng *et al.*, 2002a). To obtain a closed expression for  $\alpha_b$ , the above quantities are evaluated directly within a statistical model for the bubble dynamics. Two quantities define this model: the bubble velocity and the bubble merger criteria. The bubble velocity is defined as the sum of a single (periodic array) bubble velocity and a bubble interaction term, the “envelope velocity.” The bubble velocity as a sum of these two terms has been tested against simulation data. The criteria for bubble merger is defined to be the time at which the retarded bubble starts to move backwards, using this two-term formula for the bubble velocity. Note that the bubble interaction term can have either sign, so that a zero total velocity is possible. The bubble merger criteria was shown to be an insensitive parameter in the model.

From these two inputs,  $\omega$  and  $h'_m$  are determined. The result is the determination  $\alpha_b \approx 0.5\text{--}0.6$ , in agreement with

experimental results. The same formulas yield the bubble height-to-width ratio, cited in Table 1. Since (1) depends on two parameters, it is important to check it (as we do) on two independent sets of data. Specifically,  $\omega$  is very sensitive to the bubble width whereas  $\alpha_b$  can mask canceling errors between  $\omega$  and  $h'_m$ .

### 3. COMPRESSIBLE MIXING ZONE DYNAMICS

The bubble merger model is readily extended to compressible flow. The single bubble velocity,  $c_b$  in scaled variables, must be determined for compressible flow. This quantity affects the envelope velocity and thus the total bubble velocity. The remainder of the analysis is unchanged. See Chen *et al.* (1993). This same reference shows that  $\alpha_b$  increases with increasing values of the dimensionless compressibility  $\lambda g/c_b^2$ . It was also shown that the bubble merger model predictions for  $\alpha_b$ , as corrected in this manner for compressibility, were in good to moderate agreement with simulation results.

### 4. CENTER OF MASS MOTION

For steady acceleration (Rayleigh–Taylor) incompressible mixing, the center of mass  $Z_{COM}$  of the mixing zone satisfies  $Z_{COM} = \alpha_{COM} Ag t^2$ , in accordance with the self-similar scaling of the flow.  $Z_{COM} \approx 0$  for Atwood numbers  $A < 0.8$ . For general values of  $A$ , the scaling law  $\alpha_{COM} = const.A^\gamma$  fits the data. Here the constant is determined by the known value  $\alpha_s = 1/2$  for  $A = 1$  (free fall) and an assumed value for  $\alpha_b$ , whereas  $\gamma \approx 10$  is insensitive to the data. Thus  $Z_{COM}$  and  $\alpha_{COM}$  very efficiently constrain the self-similar flow. The COM relation introduces a new equation that establishes a link between the bubble and spike mixing growth rates. Given a value for  $\alpha_{COM}$ , we have determined that the ratio  $\alpha_s/\alpha_b$  is a solution of a quadratic equation. Thus spike data can be predicted from a knowledge of bubble data. See Glimm *et al.* (1999) and Cheng *et al.* (1999, 2000). See Figure 1.

### 5. BUOYANCY DRAG EQUATIONS

A number of authors have considered buoyancy drag equations to describe the dynamics of the edge of the mixing zone. These equations are fundamental for all models of mix, as the data they supply is of such basic importance. Our version of these equations has fewer parameters and greater predictive power than similar equations introduced by others. See Cheng *et al.* (2000). In addition, we have a finite drag coefficient in the limit  $A = 1$ , as is required on intuitive grounds. The equations have the form

$$(\rho_i + k_i \rho_{i'}) \frac{dV_i}{dt} = (\rho_i - \rho_{i'})g(t) - (-1)^i \frac{C_i \rho_{i'} V_i^2}{|Z_i|}. \tag{2}$$

**Table 1.** Bubble height-to-width ratios in experiments and models

Cheng <i>et al.</i> (2002a): Model	3
Oron <i>et al.</i> (2001): Model	1–1.5
Smeeton and Youngs (1987): Experiment	3.3
Dimonte and Schneider (1996): Experiment	2–4

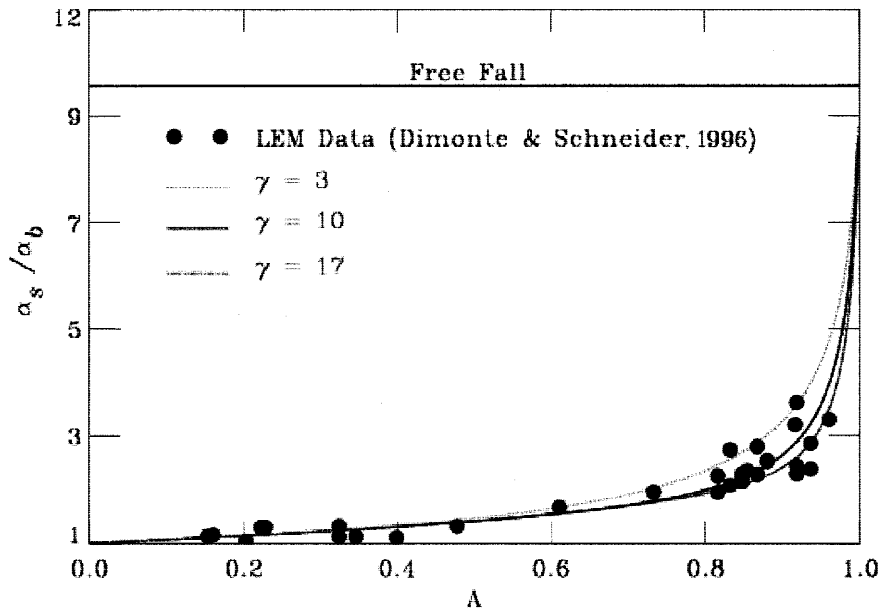


**Fig. 1.** The ratio  $\alpha_s/\alpha_b$  is determined by a COM assumption and compared to the experimental data of Dimonte and Schneider (2000) and to a power law fit. The power law is unphysical for  $A = 1$ , and thus this fit fails to reproduce the experimental data for large  $A$ . Our values for  $\alpha_s/\alpha_b$  agree with the experimental data for all values of  $A$ .

Note that the density  $\rho_i$  in the drag term in (2) is the density of the fluid being displaced. This form of drag is taken by classical text books in fluid dynamics, but has been incorrectly replaced by  $\rho_i$ , the density of the displacing fluid, by a number of workers, leading to a divergent drag coefficient in the limit  $A \rightarrow 1$ .

Here  $k_i = 1$  is an added mass coefficient,  $Z_i$  is the penetration distance of the mixing zone on side  $i = 1$  (bubble) and  $i = 1$  (spike),  $V_i$  is the edge velocity, and  $C_i$  is the drag coefficient. Also  $g(t)$  is the acceleration.

There is only one undetermined parameter in (2), namely,  $C_1$  (as  $C_2$  is determined from  $C_1$  by the COM theory).  $C_i$  itself is determined from our bubble merger model, or simulations, or from experiment. Substituting the  $h_i = \alpha_i Agt^2$  late time asymptotic solution for RT mixing, we can determine  $\alpha_i$  uniquely in terms of  $C_i$  and conversely. Thus the equation is completely determined by the RT data, and in view of Section 4, it is uniquely determined in terms of the RT bubble data alone (with exceptions noted above for large  $A$ ).

Thus (2) can be used to predict Richtmyer–Meshkov (RM) mixing rate exponents  $\theta_i$ . The late time RM asymptotics are predicted for the first time from the  $\alpha_i$  and usually from  $\alpha_b$  alone. We obtain a zero parameter agreement with experiment and with known  $A = 1$  spike limits. See Cheng *et al.* (2000) and Figure 2.

For  $g(t) = g$ , a constant (steady RT mixing), the large time asymptotic solution of the buoyancy drag equation (2) is  $|Z_i| = \alpha_i Agt^2$ . The equation cannot be integrated in closed form for general  $t$ , but a closed form approximate evaluation of the next two lower orders (the term proportional to  $t$  and the constant term) was obtained. The result exhibited an

explicit dependence of these lower order terms on the initial conditions, in contrast to the leading order asymptotics, which is independent of initial conditions. The result is

$$|Z_i(t)| = \alpha_i Ag(t - t_0)^2 + \beta_i \sqrt{\alpha_i Ag |Z_{i0}|} (t - t_0) + \gamma_i |Z_{i0}|, \quad (3)$$

where  $Z_{i0}$  is an initial amplitude, and  $V_{i0}$  is an initial velocity. We also define  $a_i = 1/(2\sqrt{\alpha_i})$  and  $f_{i0} = (1 - a_i |V'_{i0}|)/(1 + a_i |V'_{i0}|)$  as a transform of the scaled initial velocity  $V'_i = V_i/\sqrt{Ag|Z_i|}$ . Then with

$$\delta_i = \frac{2(1 + f_{i0}) - \alpha_i(1 + 3f_{i0})}{(1 + f_{i0})(1 - \alpha_i)}, \quad (4)$$

a computation shows that  $\beta_i = 2\delta_i$  and  $\gamma_i = \delta_i^2$ . Note the explicit dependence on initial conditions in the lower rather than leading order terms.

This analysis allows an improved fit and interpretation of experimental data. For example, the data of Smeeton and Youngs (1987) and of Read (1984) can be reliably distinguished from the leading order asymptotics and the dependence of this data on  $Z(t = 0)$  or  $V(t = 0)$  can be observed. See Figure 3.

Speculations concerning the cause of discrepancy between simulation and experiment have focused on three possible explanations: (a) numerical diffusion in the untracked simulations, (b) preasymptotic behavior in the simulations, and (c) noise in the experiments of a specific spectral power that generates  $t^2$  modification to the  $t^2$  experimental data. Issue (a) is in fact a sufficient explanation (see George *et al.*, 2002). It is possible that (b) may be a contributing explanation. To explore this possibility, the preasymptotic

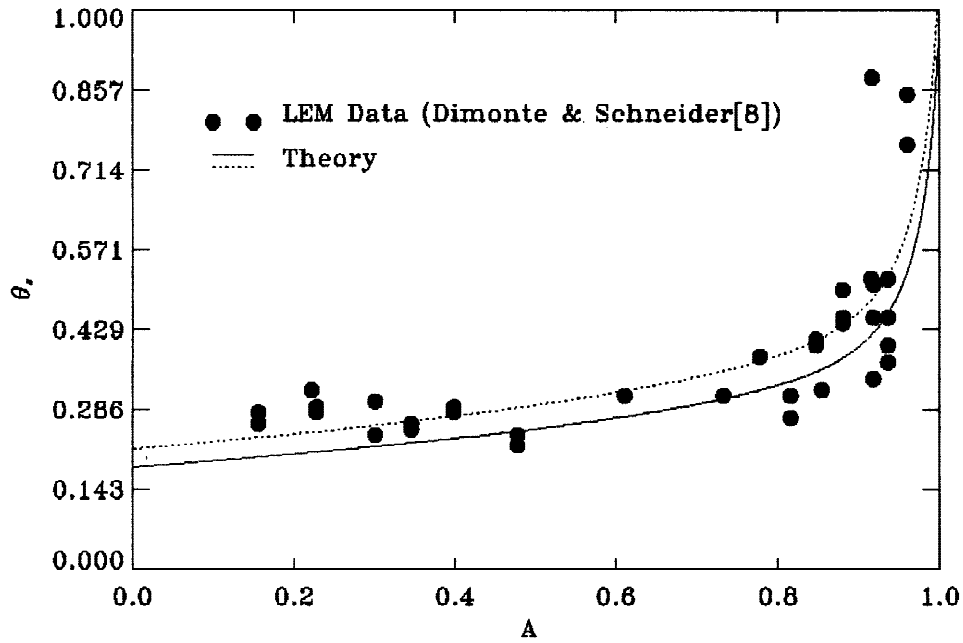


Fig. 2. The exponent  $\theta_s$  for RM mixing. The solid and dotted lines are the predictions of Cheng *et al.* (2000) for  $\alpha_b = 0.05$  and for  $\alpha_b = 0.06$ , respectively. The solid dots are LEM experiments of Dimonte and Schneider (1996).

solutions (3) of (2) will be helpful. Issue (c) is discussed in Glimm *et al.* (2001).

6. MIX MODEL EQUATIONS

Two phase flow equations appropriate to a chunk mix regime have been proposed and studied in detail (see Glimm

*et al.*, 1998, 1999, and related papers). The model has several attractive features: it is mathematically stable, that is, totally hyperbolic with real characteristics for time propagation. The equations are thermodynamically determinate, using equation of state models for each constituent in an unmixed mode. Commonly used mix models fail one or both of these properties. In fact, a thermodynamically de-

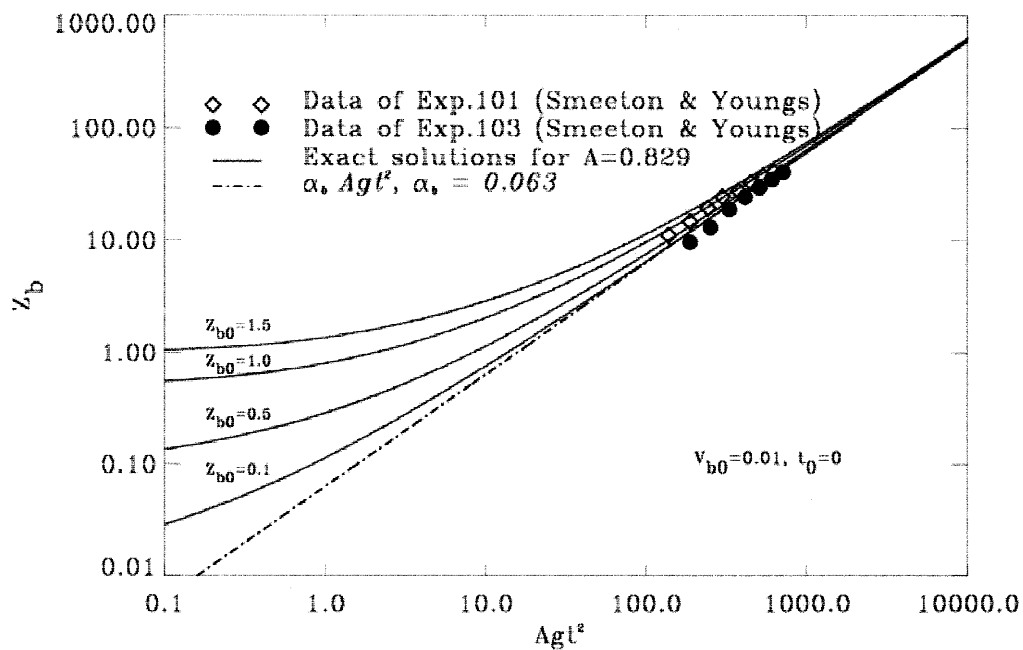


Fig. 3. Dependence of the exact solution of Eq. (1) on variation of the initial data  $Z_{b0}$ . The best fitting value for the data of Smeeton and Youngs (1987) is  $Z_{b0} = 0.75$  for their experiment number 101.

terminate set of equations is often achieved by assumption of molecular mix, leading to models that possess a single temperature.

The chunk mix equations have been analyzed in great detail, with closed form solutions obtained for the incompressible limit (Glimm *et al.*, 1998, 1999). Perturbation terms in the weakly compressible limit have been computed in closed form through second order in the Mach number (Glimm & Jin, 2001; Jin, 2001). This is the order for which the incompressible pressure first appears. Results for the volume fraction in this limit are displayed in Figure 4.

Here we discuss new insight regarding closure that have emerged from a study of the weakly compressible theory. The equations resemble the Euler equations for each fluid considered separately. They are coupled through three interface terms. Two of these are a term  $p^* \partial \beta_k / \partial z$  added to the momentum equation for species  $k$  and a term  $(pv)^* \partial \beta_k / \partial z$  is added to the energy equation, also for species  $k$ . Here  $\beta_k$  is the volume fraction of species  $k$ . We use the notation  $X^*$  to denote the quantity  $X$  averaged over the interface, and  $X_k$  to denote a volume average of  $X$  over the phase volume occupied by species  $k$ . Closure assumptions, such as neglect of Reynolds stress terms within a single species phase average, and an assumed identity of volume and mass weighted averages within a single phase average are discussed in Glimm *et al.* (1998) and earlier papers. The third interface term occurs in the (new) interface equation

$$\frac{\partial \beta_k}{\partial t} + v^* \frac{\partial \beta_k}{\partial z} = 0. \tag{5}$$

The important closure relations are those for the interface quantities  $p^*$  and  $(pv)^*$  and  $v^*$ . The closure for  $(pv)^*$  is highly constrained in terms of the  $v^*$  and  $p^*$  closures. These two are also constrained to be convex combinations of the corresponding phase quantities,  $v_k$  and  $p_k$ , with convex coefficients  $\mu_k^x$ ,  $x = v, p$ . We make the hypotheses (appropriate for a chunk mix regime) that there are no internal length scales within the mixing layer, so that the  $\mu$ s must be functions of dimensionless variables, such as  $\beta_k$ . Taking the functional dependence to be fractional linear in  $\beta_k$ , all but one of the four parameters in the fractional linear dependence is determined in an obvious manner by the boundary conditions at  $z = Z_k$ , the edges of the mixing zone. In this way the closure is mainly driven by directly observable data, a feature that the authors regard as highly desirable. In fact the edges  $Z_k$  are determined by the buoyancy equation (2). The closure relation for  $p^*$  is set in terms of the ratio of densities (Glimm *et al.*, 1998; Glimm & Jin, 2001). We now discuss the  $v^*$  closure relation, that is, the equation for the fractional linear definition of  $\mu_k^v$  in

$$v^* = \mu_2^v v_1 + \mu_1^v v_2. \tag{6}$$

After inserting obvious mixing zone boundary constraints, and our assumed form  $\mu_k^v$ , we have

$$\mu_k^x = \frac{\beta_k}{\beta_k + c_k^x(t) \beta_k}, \quad x = v, p. \tag{7}$$

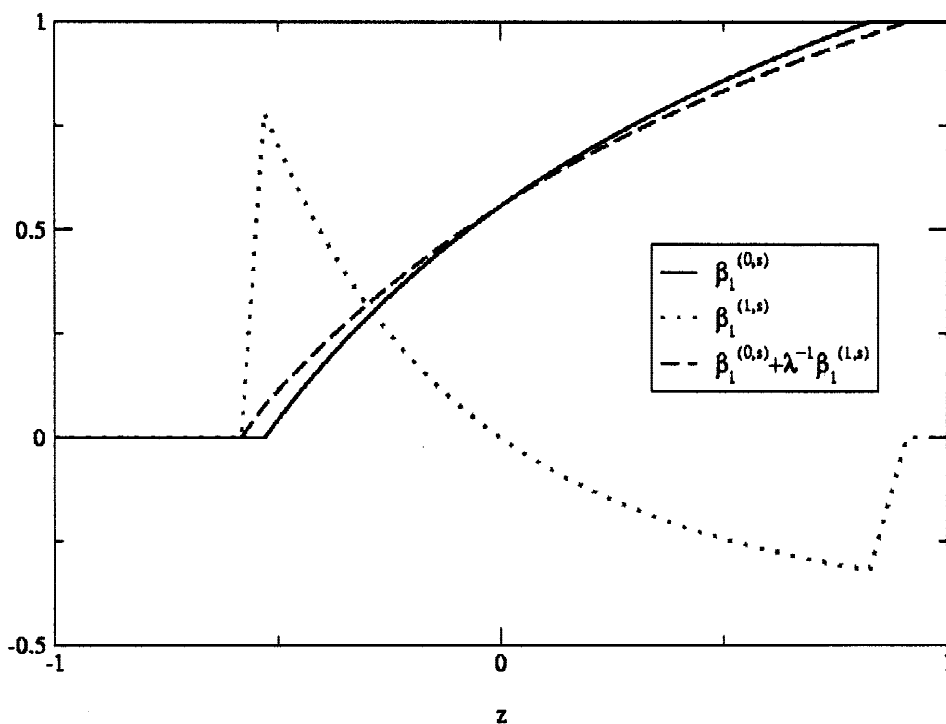


Fig. 4. Volume fraction of the light fluid, showing the incompressible solution, a perturbation term, and the compressible solution computed perturbatively through first order.

$c_k^v$  was interpreted as a ratio of the volumetric growth rates for the mixing zone for the two phases,  $c_k^v = |V_{k'}/V_k|$ , in the incompressible case (Glimm *et al.*, 1998, 1999). Here  $V_k = \partial Z_k/\partial t$ . As is observed below, both the convex sum property (6) and the fractional linear form (7) for the convex coefficients can be derived from the primitive equations, and are thus independent of closure assumptions. Closure thus is a specification of  $c_k^v$ .

The volumetric mixing rate constraint determining the  $v^*$  closure has been extended to the fully compressible case (Glimm & Jin, 2001). Because of compressibility, new terms enter into the phase volume growth rates, including the compressibility of the two phases. In dimensionless terms, this influence enters as a ratio of the sound speeds for the two fluids in the weakly compressible limit. We start with an exact identity for  $c_k^v$ , valid for the fully compressible two-fluid equations, derived in the absence of any closure assumptions at all. Note that the interface equation, the convex sum property for  $v^*$ , and the fractional linear form for  $\mu_k^v$  are all *derived* in this equation independently of closure assumptions. We have

$$c_k^v = \frac{\frac{\partial v_{k'}}{\partial z} + \frac{1}{\rho_{k'}} \frac{D_{k'} \rho_{k'}}{Dt}}{\frac{\partial v_k}{\partial z} + \frac{1}{\rho_k} \frac{D_k \rho_k}{Dt}} \tag{8}$$

is the ratio of logarithmic rates of volume creation for the two species, where  $D_k/Dt = \partial/\partial t + v_k \partial/\partial z$  is the convective derivative defined by the velocity  $v_k$ . Then the closure (absence of internal length scales) can be interpreted as an equation for  $c_k^v$ , namely,

$$\frac{\partial c_k^v}{\partial z} = 0. \tag{9}$$

It is of interest to analyze the  $v^*$  closure in the weakly compressible perturbative analysis. There we find that the incompressible pressures, the ratios of the compressible sound speeds, the second order contribution to the phase volume expansion ratio  $|V_{k'}/V_k|$ , and the second order perturbation term in the expansion of  $c_k^v$  are linked by a newly derived equation (Glimm & Jin, 2001; Jin, 2001). This equation removes an indeterminacy in the incompressible equations, previously not understood, and shows that the two phase incompressible equations, in contrast to the single phase case, remember the compressible fluids from which they are derived. We first reformulate (9) as

$$c_k^v = \frac{\int_{Z_k}^{Z_{k'}} \left( \frac{\partial v_{k'}}{\partial z} + \frac{1}{\rho_{k'}} \frac{D_{k'} \rho_{k'}}{Dt} \right) dz}{\int_{Z_k}^{Z_{k'}} \left( \frac{\partial v_k}{\partial z} + \frac{1}{\rho_k} \frac{D_k \rho_k}{Dt} \right) dz}. \tag{10}$$

The formula (10) can now be expanded perturbatively in powers of the Mach number, and the second-order term in this expansion includes the incompressible pressure. The resulting equation is the desired new equation for the incompressible pressure. See Jin (2001) and Glimm & Jin (2001).

On the basis of the above analysis, we are able to link the phenomenological drag coefficients in the buoyancy drag equation for the edge motion with fundamental laws of physics. Newton’s law of acceleration, applied at the edge of the mixing zone is equivalent to the momentum equation, evaluated at this location. The equations can be highly simplified in this evaluation (Glimm *et al.*, 1999) and resemble buoyancy drag equations (2). In fact, they are different, due to the absence of phenomenological quantities. Thus the added mass and the drag are replaced by exact quantities, which, however, are not convenient to evaluate. Specifically they relate to the pressure difference between the phases and the gradient of the pressure difference. A closed form solution for the pressure equation in the incompressible limit, to be published, reveals terms that can be readily identified as inertial terms (added mass), fundamentally exact drag terms (depending on velocity differences), and pressure difference terms (interpreted as phenomenological corrections to the drag terms). Thus we see that the buoyancy drag equations can be obtained via a closure relation that expresses the added mass and drag as pressure difference terms in the exact momentum equation and relates these to quantities known in the buoyancy drag equation, namely, lengths, velocities, and accelerations.

### 7. EFFECTIVE DIFFUSION AND REYNOLDS STRESS

Reduced multiphase mixture models have fewer equations and fewer variables. They are logically derived from more complete models. Here we derive a single-velocity, single-temperature model from the chunk mix model of Section 6, following Cheng *et al.* (2002b). For models with a single velocity, this velocity will express mean fluid flow, and cannot drive the mixture process, which is then modeled as a diffusion process. The point is to determine the (time and spatially dependent) interspecies diffusivity, which governs the mixing rates diffusivity. Assuming this to be a function of the volume fraction  $\beta_k$ , Alon and Shvarts (1996) propose diffusion proportional to  $\beta_k(1 - \beta_k) = \beta_1\beta_2$ . We find corrections to this form that reflect the deviation of the volume fraction from being a linear function of  $z$ .

The key to the computation of the diffusivity is a determination of entrainment time. For a given parcel of fluid  $k$  at a given space time location within the mixing zone, the entrainment time is defined to be (the earlier) time at which that parcel entered the mixing zone. Given the velocity history of the two phases, available in closed form (in terms of the edge positions  $Z_k$ ), one integrates backward in time until the moving edge  $Z_{k'}(s)$  is encountered. This motion is then interpreted as a diffusion process, and the exact value of

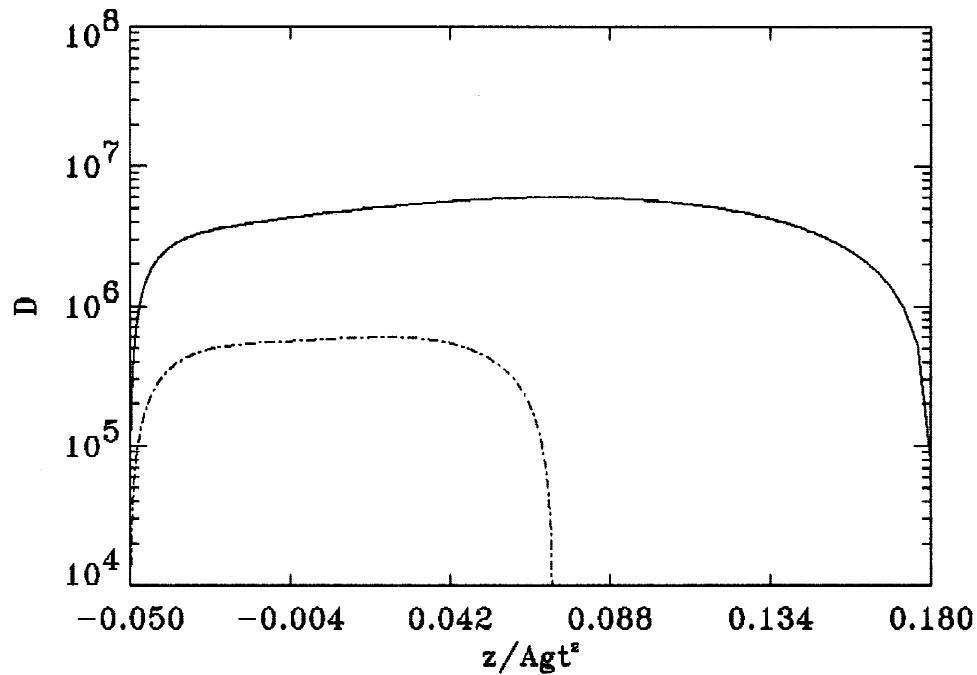


**Fig. 5.** The diffusion coefficient  $D$  across the mixing layer in RT mixing. The dash-dotted line is for  $A = 0.5$ ,  $\alpha_2 = 0.07$  and the solid line is for  $A = 0.96$ ,  $\alpha_2 = 0.18$ .

diffusion that duplicates this motion is determined. For RT mixing, the diffusivity can be determined in closed form, whereas for RM mixing, the diffusivity is solved via an approximate closed-form expression, and also by integration of an ordinary differential equation. For the general case, the solution is given up to a quadrature. For the RT case, the closed-form expression for the diffusivity  $D$  is

$$D = 2A^2 g^2 t^3 \beta_1 \beta_2 \alpha_1^2 \alpha_2^2 \left[ \frac{\beta_1^2 \alpha_1}{\alpha^3} + \frac{\beta_2^2 \alpha_2}{\alpha^3} \right],$$

where

$$\alpha = \alpha_1 \beta_1 + \alpha_2 \beta_2.$$

Note that the formula is not symmetric between  $\beta_1$  and  $\beta_2$  because  $\alpha_1 \neq \alpha_2$  for  $A > 0$ . The factor in the square brackets is the correction to the formula of Alon and Shvartz (1996). This factor reflects the lack of symmetry between the two phases and is especially significant for Richtmyer–Meshkov mixing (see Fig. 5).

The dominant component  $R_{zz}$  of the Reynolds stress tensor is also determined in Cheng *et al.* (2002b).

## 8. CONCLUSIONS

Theory has been shown to be remarkably successful for the study of turbulent mix. Zero parameter models of the compressible mixing zone have been derived from totally theoretical considerations, and match experiment quantitatively.

Both mixing zone edges and the mixing zone interior flow variables have been modeled. The latter are described by a new set of averaged equations, with several pleasant properties, including stability at a hyperbolic level of time propagation, and multispecies thermodynamics. Simpler models, such as turbulent diffusive mixing, have been derived from these equations. Details of the weakly compressible limit for our averaged equations have been solved in closed form.

## REFERENCES

- ALON, U. & SHVARTS, D. (1996). Two phase flow model for Rayleigh–Taylor and Richtmyer–Meshkov mixing. In *Proc. Fifth Int. Workshop for Compressible Turbulent Mixing*, pp.14–22. Singapore: World Scientific.
- CHEN, Y., DENG, Y., GLIMM, J., LI, G., SHARP, D.H. & ZHANG, Q. (1993). A renormalization group scaling analysis for compressible two phase flow. *Phys. Fluids A*, **5**, 2929–2937.
- CHENG, B., GLIMM, J., SALTZ, D. & SHARP, D.H. (1999). Boundary conditions for a two pressure two phase flow model. *Physica D*, **133**, 84–105.
- CHENG, B., GLIMM, J. & SHARP, D.H. (2000). Density dependence or Rayleigh–Taylor and Richtmyer–Meshkov mixing rates. *Phys. Lett. A* **268**, 366–374.
- CHENG, B., GLIMM, J. & SHARP, D.H. (2002a). A three-dimensional renormalization group bubble merger model for Rayleigh–Taylor mixing. *Chaos* **12**, 267–274.
- CHENG, B., GLIMM, J. & SHARP, D.H. (2002b). Multi-temperature multi-phase flow model. *Zeitschrift für Angewandte Mathematik und Physik*, **53**, 211–238.

- DIMONTE, G. & SCHNEIDER, M. (1996). Turbulent Rayleigh–Taylor instability experiments with variable accelerations. *Phys. Rev. E* **54**, 3740–3743.
- DIMONTE, G. & SCHNEIDER, M. (2000). Density ratio dependence of sustained acceleration histories. *Phys. Fluids* **12**, 304–321.
- GEORGE, E. GLIMM, J., LI, X.L., MARCHESE, A. & XU, Z.L. (2002). A comparison of experimental, theoretical, and numerical simulation of Rayleigh–Taylor mixing rates. *Proc. Natl. Acad. Sci. USA* **99**, 2587–2592.
- GLIMM, J., GROVE, J., LI, X., OH, W. & SHARP, D.H. (2001). A critical analysis of Rayleigh–Taylor growth rates. *J. Comp. Phys.* **169**, 652–677.
- GLIMM, J. & JIN, H. (2001). An asymptotic analysis of two-phase fluid mixing. *Bol. Soc. Bras. Mat.* **32**, 213–236.
- GLIMM, J., SALTZ, D. & SHARP, D.H. (1998). Two-pressure two phase flow. In *Nonlinear Partial Differential Equations*. pp. 124–128. Singapore: World Scientific. pp. 124–148.
- GLIMM, J., SALTZ, D. & SHARP, D.H. (1999). Two phase modeling of a fluid mixing layer. *J. Fluid Mech.* **378**, 119–143.
- GLIMM, J. & SHARP, D.H. (1990). Heater mixing as a renormalization group fixed point. *Phys. Rev. Lett.* **64**, 2137–2139.
- GLIMM, J. & SHARP, D.H. (1997). Stochastic partial differential equations: Selected applications in continuum physics. In *Stochastic Partial Differential Equations: Six Perspectives*. Providence: American Mathematical Society.
- JIN, H. (2001). The incompressible limit of compressible multi-phase flow equations. Ph.D. Thesis. Stony Brook, NY: University at Stony Brook.
- ORON, D., ARAZI, L., KARTOON, D., RIKANATI, A. ALON, A. & SHVARTS, D. (2001). Dimensionality dependence of Rayleigh–Taylor and Richtmyer–Meshkov instability late time scaling laws. *Phys. Plasmas* **8**, 2883–2889.
- READ, K.I. (1984). Experimental investigation turbulent mixing by Rayleigh–Taylor instability. *Physica D* **12**, 45–58.
- SHARP, D.H. & WHEELER, J.A. (1961). Late stage of Rayleigh–Taylor instability. Institute for Defense Analysis.
- SMEETON, V.S. & YOUNGS, D.L. (1987). Experimental investigation of turbulent mixing by Rayleigh–Taylor instability (Part 3). Report number 0 35/87. Atomic Weapons Establishment, Aldermaston, UK.